

**CENTRIFUGE MODELING OF STEEL CATENARY RISERS IN THE
TOUCHDOWN ZONE**

by

© Bradley James Elliott

**A thesis submitted to the
School of Graduate Studies
in partial fulfillment of the
requirements for the degree of
Masters of Engineering**

**Faculty of Engineering and Applied Science
Memorial University of Newfoundland
August 2012**

St. John's

Newfoundland

Canada

ABSTRACT

Field surveys of installed catenary risers have shown the creation of deep trenches cut into the seabed around the touchdown point. This section is a critical to the fatigue life of Steel Catenary Risers (SCRs) as it consists of a repetitive complex fluid-riser-soil interaction and often contains the maximum deflection and bending moment. Current practice and design programs typically assume a flat, rigid, “non-interacting” seabed and do not account for the complex nonlinear processes associated with the repetitive interaction of the riser with the seabed and trench formation. An important step forward in the state-of-the-art would therefore be to improve the fluid-riser-soil interaction models that are currently used in the analysis and design procedures for steel catenary risers.

The thesis presented herein focuses on the development of a novel centrifuge experimental tool for modeling a 0.5 m outside diameter, 108 m long steel catenary riser at the touchdown zone and to investigate the trench formation mechanism arising from the fluid-riser-soil interaction and its influence on the fatigue stresses. This thesis provides the details of a SCR model developed for the geotechnical centrifuge at C-CORE, the associated scaling laws, and the results of two series of physical tests along with the confirmatory finite element analyses. Further, it discusses the current status of the state-of-the-art on steel catenary riser modeling at the touchdown zone, identifies the knowledge gaps, and provides recommendations for future research based on physical and numerical models.

The results of the physical tests indicated that the SCR model was consistent with engineering theory and centrifuge scaling laws, verified using finite element analysis. It was also demonstrated that there was a considerable reduction in bending and tensile fatigue stresses due to the change of trench geometry and the increase in trench depth from its original mudline state, potentially increasing the fatigue life of the SCR.

To my wife, Penney Elliott

ACKNOWLEDGEMENTS

The completion of this research and thesis was made possible by the generous contributions made by C-CORE and its employees. I would like to thank C-CORE for providing this opportunity and the encouragement to pursue a Master's degree in Engineering. A special thanks to Gerry Piercey and John Barrett for their technical support and guidance.

I would also like to acknowledge my supervisors, especially Dr. Bipul Hawlader and Dr. Arash Zakeri. Their continuous motivation and advice made this research a success. It was a privilege to be their student.

Special thanks goes to my parents, Terry and Marian Elliott, and my brother, Greg Elliott, for their moral support through my engineering program, both undergraduate and post graduate.

Last, but not the least, I would like to thank my wife, Penney Elliott. Without her love, support, and patience I could not have completed this undertaking. Her encouragement helped me when completion of this research seemed unachievable.

TABLE OF CONTENTS

ABSTRACT.....	ii
ACKNOWLEDGEMENTS.....	v
LIST OF TABLES.....	x
LIST OF FIGURES.....	xi
LIST OF ABBREVIATIONS AND SYMBOLS.....	xiv
1. INTRODUCTION, OVERVIEW, AND CO-AUTHORSHIP STATEMENT.....	1-1
1.1. INTRODUCTION.....	1-1
1.2. OBJECTIVES AND OVERVIEW.....	1-4
1.3. CO-AUTHORSHIP STATEMENT.....	1-5
2. LITERATURE REVIEW.....	2-1
3. CENTRIFUGE MODELING OF STEEL CATENARY RISERS AT TOUCHDOWN ZONE PART 1: DEVELOPMENT OF NOVEL CENTRIFUGE EXPERIMENTAL APPARATUS.....	3-1
3.1. ABSTRACT.....	3-1
3.2. INTRODUCTION.....	3-2
3.3. LITERATURE REVIEW AND PREVIOUS EXPERIMENTAL WORKS.....	3-2
3.4. MODELING CONSIDERATIONS.....	3-6
3.4.1. Motion Inputs and Need for a Cut-Off Model.....	3-6
3.4.2. Boundary Conditions.....	3-8
3.4.3. Capability for Riser-Fluid-Soil Interaction Modeling.....	3-9
3.4.4. Centrifuge Scaling Considerations.....	3-10

3.5. EXPERIMENTAL SETUP	3-10
3.5.1. Test Box	3-11
3.5.2. Motion Actuation System: X-Z Stage	3-12
3.5.3. Model SCR	3-17
3.5.4. End Conditions	3-18
3.5.5. Instrumentation	3-20
3.6. ELASTIC SEABED TEST RESULTS	3-23
3.7. NUMERICAL MODEL OF ELASTIC SEABED TEST	3-26
3.8. CONCLUSIONS	3-30
3.9. ACKNOWLEDGEMENTS	3-30
3.10. REFERENCES	3-30
4. CENTRIFUGE MODELING OF STEEL CATENARY RISERS AT TOUCHDOWN ZONE PART II: ASSESSMENT OF CENTRIFUGE TEST RESULTS USING KAOLIN CLAY	4-1
4.1. ABSTRACT	4-1
4.2. INTRODUCTION	4-2
4.3. PHYSICAL SETUP AND DESIGN PARAMETERS	4-2
4.3.1. Model Riser Properties and Boundary Conditions	4-2
4.3.2. Riser Boundary Conditions	4-3
4.3.3. Model Seabed Preparation and Properties	4-3
4.3.4. Applied Motions	4-4
4.3.5. Instrumentation	4-7

4.3.6.	Pore Pressure Transducer.....	4-8
4.3.7.	Displacement Measurements.....	4-9
4.3.8.	Inclinometers.....	4-9
4.3.9.	Riser.....	4-9
4.4.	PROCEDURES FOR CENTRIFUGE TESTS.....	4-10
4.4.1.	Consolidation Phase.....	4-10
4.4.2.	Applied Motions.....	4-11
4.4.3.	Soil Characterization Tests.....	4-12
4.4.4.	End of Test / Post Test Measurements.....	4-12
4.5.	TEST RESULTS AND DISCUSSION.....	4-12
4.5.1.	Heave and Surge Motions.....	4-12
4.5.2.	Shear Strength of Model Seabed.....	4-13
4.5.3.	Tension Forces.....	4-16
4.5.4.	Bending Moments.....	4-18
4.5.5.	Trench Data.....	4-23
4.5.6.	Riser Inclination at Boundaries.....	4-27
4.5.7.	Pore Pressures.....	4-28
4.5.8.	Fatigue Stresses.....	4-29
4.6.	CONCLUSIONS.....	4-32
4.7.	ACKNOWLEDGEMENTS.....	4-33
4.8.	REFERENCES.....	4-33
5.	CONCLUSIONS AND RECOMMENDATIONS.....	5-1

5.1. CONCLUSIONS.....	5-1
5.2. RECOMMENDATIONS	5-3
6. REFERENCES	6-1

LIST OF TABLES

Table 2-1: Geotechnical properties of seabed clay at the Watchet Harbour (Bridge and Willis, 2002)	2-1
Table 2-2: Test rig setup and riser actuation details (Bridge and Willis, 2002)	2-3
Table 3-1: Scaling laws (after Taylor, 1995)	3-10
Table 3-2: Summary of riser model and equivalent prototype dimensions	3-18
Table 4-1: Riser strain gauge locations	4-10
Table 4-2: Testing sequence	4-11

LIST OF FIGURES

Figure 1-1: General catenary riser arrangement (after Bridge et al., 2003).....	1-2
Figure 2-1: Test setup overview of STRIDE project (after Bridge et al., 2003)	2-2
Figure 2-2: Test setup schematic of STRIDE project (after Bridge et al., 2003)	2-2
Figure 2-3: CARISMA test rig setup (Sintef, 2001).....	2-5
Figure 2-4: Riser-soil interaction model (Bridge et al., 2004).....	2-7
Figure 3-1: Schematic of prototype SCR with sectional SCR concept	3-7
Figure 3-2: Centrifuge test setup.....	3-11
Figure 3-3: X-Z stage.....	3-13
Figure 3-4: Typical riser motion.....	3-15
Figure 3-5: Holding accuracy of riser (Note: the surge displacement magnitudes have been exaggerated 10 times for clarity).....	3-16
Figure 3-6: Sample of 1 Hz motions on 0.05 Hz carrier.....	3-16
Figure 3-7: Motion-end of model SCR.....	3-19
Figure 3-8: Fixed-end of model SCR.....	3-19
Figure 3-9: Instrumentation layout	3-21
Figure 3-10: Laser system and model SCR on elastic seabed	3-22
Figure 3-11: Heave input with corresponding tension values	3-24
Figure 3-12: Bending moment profile for 401.1 N tension	3-24
Figure 3-13: Bending moment profile for 660.6 N tension	3-25
Figure 3-14: Bending moment profile for 90.7 N tension	3-25
Figure 3-15: Comparison of physical and FEA for 401.1 N tension.....	3-28

Figure 3-16: Comparison of physical and FEA for 660.6 N tension.....	3-29
Figure 3-17: Comparison of physical and FEA for 90.7 N tension.....	3-29
Figure 4-1: Motions used in centrifuge test: M1 (a), M2 (b), M3 (c), and M4 (d).....	4-6
Figure 4-2: Heave versus surge displacements: M3 motion (a) and M4 motion (b).....	4-7
Figure 4-3: Instrumentation layout with clay bed.....	4-8
Figure 4-4: Applied motions.....	4-13
Figure 4-5: Undrained shear strength (a) and water content (b) profiles in model terms (note: zero on the y-axis corresponds to mudline).....	4-15
Figure 4-6: Tension of SG1 (a) and SG21 (b) during applied motions. From the left, each three sets represent M1, M2, M3, M4 and M2 motions, respectively.	4-17
Figure 4-7: Response of bending strain gauges (note: scale of Y axes may be different). From the left, each three sets represent M1, M2, M3, M4 and M2 motions, respectively.	4-20
Figure 4-8: Bending moment profiles before and after motions.....	4-21
Figure 4-9: Bending moments measured by SG10 during M1 motion (a), and SG10 bending moment difference between consecutive maxima and minima versus number of cycles in all motions (b)	4-22
Figure 4-10: Laser measurements versus number of applied cycles	4-24
Figure 4-11: Three-dimensional view of the final trench geometry (color bar indicate depth in mm).....	4-25

Figure 4-12: Plan views of final trench geometry. Zero corresponds to the fixed-end. Lasers were located 800 mm and 1,600 mm from the fixed-end. The legend is in model terms. For conversion one needs to multiply by 40.	4-26
Figure 4-13: Final trench base and berm height profiles	4-27
Figure 4-14: Riser inclination data at the motion-end with positive showing clockwise rotation (a) and at the fixed-end (b)	4-28
Figure 4-15: Difference between maxima and minima tensions in SG1 versus number of cycles (a) and tensile stresses versus number of cycles (b)	4-30
Figure 4-16: Difference between consecutive maxima and minima bending stresses in SG10 versus number of applied cycles	4-32

LIST OF ABBREVIATIONS AND SYMBOLS

CARISIMA	Catenary Riser-Soil Interaction Model for Global Riser Analysis
CMM	coordinate measuring machine
CNC	computer numerical control
DC	direct current
FE	finite element
FEA	finite element analysis
JIP	joint industry project
LDT	linear displacement transducer
LVDT	linearly variable differential transducer
OTC	Offshore Technology Conference
PPT	pore pressure transducer
PTFE	polytetrafluoroethylene
RAO	response-amplitude-operator
ROV	remotely operated vehicle
SCR	steel catenary riser
SG	strain gauge
STRIDE	Steel Risers In Deepwater Environments
TDP	touch down point
TDZ	touch down zone
VIV	vortex induced vibrations
WD	water depth
Z	section modulus
c_v	coefficient of consolidation
w	moisture content
ρ	bulk density
ρ_d	dry density
ρ_s	particle density
w_L	liquid limit

w_p	plastic limit
I_p	plasticity index
G_s	specific gravity
s_u	undrained shear strength
$s_{u, \text{undisturbed}}$	undisturbed shear strength
$s_{u, \text{remoulded}}$	remoulded shear strength
m_v	coefficient of volume compressibility

1. INTRODUCTION, OVERVIEW, AND CO-AUTHORSHIP STATEMENT

1.1. INTRODUCTION

Catenary risers, steel and flexible, are an advancing technology for offshore oil and gas production. A riser is a long pipe that freely hangs from a floating production platform or vessel and gently curves down to the seabed where it connects to a wellhead, a production unit, or a network of pipelines. Steel Catenary Risers (SCRs) are long steel pipes used in medium and particularly deep (>300 m) water depths (WD), with minimum depths governed on the bend radius of the riser. SCRs are advantageous over the conventional flexible risers since they can be suspended in longer lengths without the need for mid-depth arches or buoys. They can also be operated at pressures, temperatures, and diameters that cannot be achieved by flexible pipe, allowing use of a smaller number of larger diameter lines. Furthermore, SCRs are more adaptable for design purposes and due to their simplicity, have better availability and are less costly than flexible risers (Howells, 1995). During normal operating conditions, SCRs are connected to a floating platform or vessel via a flex-joint or a taper-stress-joint (steel or titanium) to absorb the dynamic loads resulting from large angular movement of the system. SCRs may be described as consisting of three sections as shown in Figure 1-1, below (Bridge et al., 2003):

- Catenary zone: where the riser hangs in a catenary section;
- Buried zone: where the riser is within an open trench or buried in soil; and
- Surface zone: where the riser rests on the seafloor.

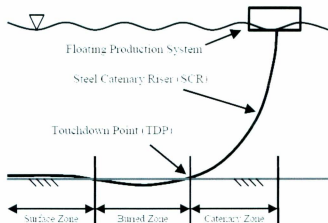


Figure 1-1: General catenary riser arrangement (after Bridge et al., 2003)

Beyond the Touchdown Point (TDP), SCRs tend to trench and bury themselves within the 'buried zone' under the loads arising from the self-weight, platform motions, and current. The main platform motions are as follows (Bridge et al., 2003):

- First order motions: caused by wave action on the vessel and are of high-frequency type such as heave, surge, and sway;
- Second order motions: caused by wind gusts and are of low-frequency type. They are often referred to as the 'slow drift motions'; and
- Translational: displacements caused by the mean of environmental actions such as current, wind, and wave as well as system failure (e.g. mooring failure).

The current loads that act directly on SCRs are of drag and high frequency motions resulting from Vortex Induced Vibrations (VIV). Typically, the maximum fatigue

damage resulting from VIV occurs at the TDP where the tension is lowest (Thethi and Moros, 2001). All of these loads may result in severe fatigue damage on a SCR, particularly within the buried zone near the TDP considering the soil response on the riser. This could ultimately result in failure of a SCR resulting in production downtime and environmental damage, and hence, predicting the fatigue life of SCRs is a key design issue.

Remotely Operated Vehicle (ROV) surveys of installed catenary risers, steel and flexible, have shown deep trenches cut into the seabed beyond the TDP. Trenches have been seen that are four to five pipe diameters deep and three to four pipe diameters wide, with an amount of soil backfill in the trench, even just a few months after installation. Current practice for catenary riser design takes little account of such circumstances, with Finite Element Analysis (FEA) programs typically assuming a flat, rigid, “non-interacting” seabed. The dynamic nature of deep-water SCRs connected to floating platforms suggests that such an approach may be un-conservative (Willis and West, 2001). While modeling of the seafloor soil as a linear elastic material (e.g. Pesce et al., 1998) could provide useful insights into the soil-riser interaction mechanism, full-scale model tests and field observations (Bridge et al., 2004; Bridge and Willis, 2002) show that the problem involves complex non-linear processes such as trench formation, foundation soil suction during riser breakaway, and non-linear foundation soil stiffness under the riser pushdown (Aubeny et al., 2006). Hence, an important step forward in the state-of-the-art

would be to improve the riser-soil interaction models that are currently used in the analysis and design procedures.

1.2. OBJECTIVES AND OVERVIEW

C-CORE has developed a novel apparatus with funding from industry to simulate SCRs at the TDZ in a geotechnical centrifuge. The author of this thesis had significant input and involvement in the design and fabrication of this tool. The objectives of this thesis project were:

- To test the performance of the tool and verify / validate the scaling assumptions made during its development;
- To study the fluid-riser-soil interaction and its role in trench formation; and
- To investigate the role of the trench on the fatigue stresses exerted on a SCR during various storm conditions.

This thesis was written using a manuscript style format and consists of two journal papers submitted to the Journal of Ocean Engineering on March 30, 2012. The first journal paper, presented in Section 3, describes the scaling and physical characteristics of the model with validation by comparing the results of the tool incorporating a linear elastic seabed with a finite element model. The second journal paper, Section 4, incorporated a nonlinear elastic seabed into the physical model to investigate the trench formation mechanisms and influence it has on the fatigue life of the riser. A summary of both journal papers is presented in Section 5.

1.3. CO-AUTHORSHIP STATEMENT

The author of this thesis was responsible for the development and execution of the two centrifuge tests described, as well as processing and analyzing the resulting physical data set. The author was also responsible for producing and evaluating a finite element model, interpretation of the results, and drawing conclusions and recommendations. Further, it was the author's responsibility to conduct a literature review and compose two journal papers presented in this thesis.

Dr. Bipul Hawlader (MUN), Dr. Arash Zakeri (C-CORE), and all other co-authors contributed to the review of this thesis and journal papers, as well as providing input into the focus of research.

2. LITERATURE REVIEW

A number of model tests have been directed toward understanding the fluid-riser-soil interaction mechanism of SCRs. The first was a series of full-scale truncated SCR tests carried out over a period of three months in Watchet Harbour on the west coast of England. The experimental program was part of Phase 3 in the Steel Risers in Deepwater Environments (STRIDE) Joint Industry Project (JIP) with the objectives of assessing the importance of riser-seabed interaction and developing finite element analysis techniques to match measured responses (Willis and West, 2001). The Watchet Harbour is tidal and has seabed properties similar to those of the deepwater Gulf of Mexico (Table 2-1).

Table 2-1: Geotechnical properties of seabed clay at the Watchet Harbour (Bridge and Willis, 2002)

Parameter	Value	Parameter	Value
Moisture Content, w	104.7 %	Average Organic Content	3.2 %
Bulk Density, ρ	1.46 Mg/m ³	Specific Gravity, G_s	2.68
Dry Density, ρ_d	0.73 Mg/m ³	$S_{u1 \text{ undisturbed}}$	3.5 kPa
Particle Density, ρ_s	2.68 Mg/m ³	$S_{u2 \text{ remoulded}}$	1.7 kPa
Liquid Limit, w_L	88 %	Sensitivity of Clay	3.3
Plastic Limit, w_P	39 %	Coefficient of Consolidation, c_v	0.5 m ² /year
Plasticity Index, I_P	49 %	Coefficient of Volume Compressibility, m_v	15 m ³ /MN

The riser model tested was a 110 m (360 ft) long, 0.1683 m (6-5/8 inch) diameter pipe connected to an actuator unit to simulate the wave motions of a platform in 1000 m (3,300 ft) water depth, and a seabed anchor at the opposing end, shown in Figure 2-1 and

Figure 2-2 (Bridge and Willis, 2002). The test setup and riser actuation details are given in Table 2-2.

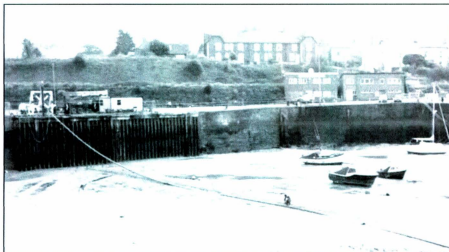


Figure 2-1: Test setup overview of STRIDE project (after Bridge et al., 2003)

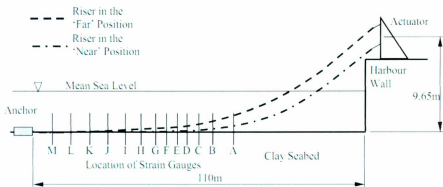


Figure 2-2: Test setup schematic of STRIDE project (after Bridge et al., 2003)

Table 2-2: Test rig setup and riser actuation details (Bridge and Willis, 2002)

Test Rig Parameter	Value	Actuation Details		
		Reference	Offshore Equivalent Motion	Travel at Actuator
Riser material	API, 5L Grade B fy = 448.2 MPa	Dynamic @ near / nominal /far	Heaving storm wave about either the 0.5 % WD near, nominal, 1.1 % far vessel position	Vertical sine wave, +/- 0.4 m, 25 second period about the - 0.4 m datum, 0m datum, +1.0 m datum
Height of nominal position above seabed	9.65 m	Lateral dynamic	Surging or swaying storm wave about nominal	Horizontal sine wave, 0 m datum, +/- 0.4 m, 18 second period
Length of chain at actuator	3.86 m	Pull-up	Spar failed mooring drift speed, near 0.8 % to far 1.4 % WD	-0.8m to +1.4m @ 0.1 m/s and 0.01 m/s
Mean water level	3.5 m	Lay-down	Spar failed mooring drift speed, far 1.4 % to near 0.8 % WD	+1.4 m to -0.8 m @ 0.1 m/s and 0.01 m/s

The tests were conducted using various seabed conditions, such as an open trench formed naturally by the riser motion, an artificially deepened trench, a backfilled trench, and a rigid seabed. The tests were also carried out both in air and water (i.e. during the tide-in and tide-out conditions). It was concluded that the soil suction force, repeated loading, pull up velocity, and the length of the consolidation time all play a key role in the fluid-riser-soil interaction. It was determined the soil suction consisted of three parts (Bridge and Willis, 2002):

- Suction mobilization: the suction force increasing from zero to maximum as the riser begins to move upwards;

- Suction plateau: the suction force remaining constant as the riser moves further upwards; and
- Suction release: the suction force decreasing from maximum with further upward movement of the riser to zero at the breakout displacement.

It was concluded that the soil suction force is independent of the consolidation time (Bridge and Willis, 2002). Willis and West (2001) back analyzed the experimental results using FEA programs such as Flexcom3-D, ABAQUS, and ANSYS, by defining specific contact elements that simulated the riser-soil interaction effects and the non-linear and hysteretic force-distance curves, known as the “backbone curves”, that are associated with the interaction between a solid member and a clay soil. The numerical analyses performed satisfactorily in modeling the riser response when compared to the field data.

Complimentary to the STRIDE Phase 3 JIP was a series of small-scale laboratory SCR tests conducted under the Catenary Riser-Soil Interaction Model for Global Riser Analysis (CARISIMA) JIP. These tests were performed in two phases: Phase 1 (14 vertical and 17 horizontal tests) was completed during spring 2000, and Phase 2 (10 vertical and 6 irregular tests) was completed during spring 2001. The clay used in the experiments was taken from a reference site in Onsoy, located southeast of Norway. In the laboratory, the clay was consolidated under dead weight for a period of approximately six weeks. The test rig was originally designed to simulate the vertical (suction) and

horizontal (pullout) motions of a SCR independently, however, in Phase 2 it was decided to modify the test setup to allow for simultaneous motion of the pipe sample both vertically and horizontally. The actuator design was capable of translating the SCR model ± 500 mm in the horizontal plane and ± 80 mm in the vertical plane. The main parameters monitored during execution of the tests (both vertically and horizontally) were loads, displacements, and accelerations (Sintef, 2001). The test rig setup is illustrated in Figure 2-3.

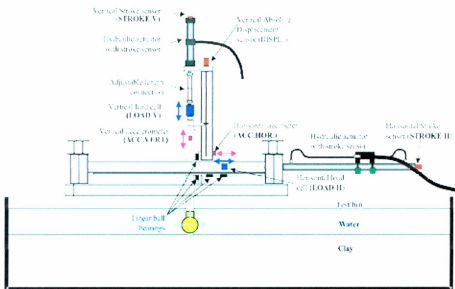


Figure 2-3: CARISIMA test rig setup (Sintef, 2001)

A numerical model was developed based on the CARISIMA test results (Bridge et al., 2004). For the vertical tests, one important observation made was that the mobilized soil

resistance was very dependent of the lift-off velocity. As part of the information/data exchange agreement between the CARISIMA JIP and the STRIDE Phase 3 JIP, full access to all test results provided further confidence in the CARISIMA numerical model through back-analysis of the STRIDE test results.

Bridge et al. (2004) developed an advanced analytical riser-soil interaction model based on the data obtained through the STRIDE and CARISIMA JIP's. Their riser-soil interaction model is based on the backbone curve concept and is illustrated in Figure 2-4. The model consisted of two scenarios, with and without soil separation. Both scenarios were based on the backbone curve concept and considered soil suction forces and soil stiffness (i.e. static stiffness and small displacement dynamic stiffness) at various stages of the interaction. The models may be used to form the basis for numerical analysis, however, the authors stated that the dynamic soil stiffness models considered are conservative since they do not account for soil softening due to repetitive cycling and use bearing load as opposed to the touchdown point (TDP) reaction force for calculating soil stiffness.

The STRIDE and CARISIMA JIP's provided valuable insight in to the riser-soil interaction mechanism based on which, a number of analytical models were developed (e.g. Aubeny and Biscontin, 2009; Nakhaee and Zhang, 2010; Randolph and Quiggin, 2009). However, these JIP's simulated only certain aspects of the riser-soil interaction mechanism. For example, movement in the surge and sway directions (i.e. horizontal)

were not simulated in the STRIDE program and the CARISIMA physical tests were mainly done with approximately 2 m straight section of 0.2 m diameter pipe. Therefore, there is need to develop a tool that can correctly simulate as many aspects of the fluid-riser-soil interaction mechanism as possible.

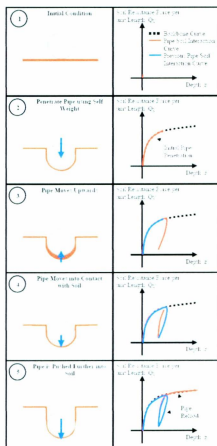


Figure 2-4: Riser-soil interaction model (Bridge et al., 2004)

To complement the CARISMA program, a series of 40 g centrifuge tests were performed using a geotechnical beam centrifuge at the National University of Singapore to simulate the repeated vertical movement of a length of riser. The model riser pipe consisted of a 300 mm long stainless steel tube with an outside diameter of 50 mm and a wall thickness of 3 mm. The ends of the tube were sealed and the model was instrumented with three pore pressure transducers (PPTs) to measure pore pressures within the soil. During the tests the pipe was subject to cyclic motion over a fixed vertical displacement amplitude from an invert embedment of 0.5 pipe diameters to 3 pipe diameters into the soil (Hu, H.J.E., 2009). The tests show that with significant progressive degradation of soil strength and diminution of excess pore pressure as the number of load cycles increases, there is a reduction in fatigue damage of the riser.

These centrifuge tests model the touchdown zone as strictly a vertical displacement of the riser and does not capture the lay down or pull off mechanism that govern this zone. Although the results are conclusive, they only focus on one aspect of the fluid-riser-soil interaction and do not capture the entire mechanism.

3. CENTRIFUGE MODELING OF STEEL CATENARY RISERS AT TOUCHDOWN ZONE PART 1: DEVELOPMENT OF NOVEL CENTRIFUGE EXPERIMENTAL APPARATUS

Submitted to: Ocean Engineering, Date of submission: March 30, 2012.

*Authors: Bradley J. Elliott, Arash Zakeri, Andrew Macneill, Ryan Phillips,
George Li, Edward C. Clukey.*

3.1. ABSTRACT

The critical location for fatigue damage in Steel Catenary Risers (SCRs) is often located within the Touchdown Zone (TDZ), where cyclic interaction of the riser with the seabed occurs. Fluid-riser-soil interaction at the TDZ is a complex phenomenon with significant room for improving the understanding of the interaction, the trench formation mechanism, and their influence on fatigue life. This paper describes a novel experimental tool developed for SCR testing in a geotechnical centrifuge. It discusses the modeling parameters, scaling considerations, and developed actuation system. Further, it presents the results of a series of trial tests done on an elastic seabed model and compares the measurements to the results of Finite Element Analysis (FEA). Finally, it discusses the potential of the tool in modeling SCRs at TDZ using seabed soil and dual frequency Response-Amplitude-Operator (RAO) motions.

3.2. INTRODUCTION

Steel Catenary Risers (SCRs) are an enabling technology for oil and gas production in deep and ultra-deep waters. Fatigue stresses due to vessel movements, vortex-induced vibrations, and interaction with the seabed in the Touchdown Zone (TDZ) are significant to their performance. The critical location for fatigue damage often occurs within the TDZ, where cyclic interaction of the riser with the seabed occurs (Aubeny and Biscontin, 2009). The understanding of the fluid-riser-soil interaction, however, is very limited; therefore, the oil and gas industry has concerns regarding the levels of conservatism and margins of safety in SCR design (Bridge et. al., 2003). This paper is part of a large research program, the results of which will be presented in two papers (i.e. Papers I and II). Part I (this paper) describes the development of the test apparatus and validation of the model. Part II presents the results of a riser model tested on a kaolin clay seabed using a series of motions in the heave and surge directions. The seabed had undrained shear strength profile similar to that encountered in deepwater Gulf of Mexico.

3.3. LITERATURE REVIEW AND PREVIOUS EXPERIMENTAL WORKS

A number of model tests have been directed toward understanding the fluid-riser-soil interaction mechanism of SCRs. The first was a series of full-scale truncated SCR tests carried out over a period of three months in Watchet Harbour on the west coast of England. The experimental program was part of Phase 3 in the Steel Risers in Deepwater Environments (STRIDE) Joint Industry Project (JIP) with the objectives of assessing the importance of riser-seabed interaction and developing Finite Element Analysis (FEA) techniques to match measured response (Willis and West, 2001). The riser model tested

was a 110 m (360 ft) long, 0.1683 m (6-5/8 inch) diameter pipe connected to an actuator unit to simulate the wave motions of a platform in 1000 m (3,300 ft) water depth, and a seabed anchor at the opposing end.

The tests were conducted using various seabed conditions, such as an open trench formed naturally by the riser motion, an artificially deepened trench, a backfilled trench, and a rigid seabed. The tests were also carried out both in air and water (i.e. during the tide-in and tide-out conditions). It was concluded that the soil suction force, repeated loading, pull up velocity, and the length of the consolidation time all play a key role in the riser-soil-water interaction. It was determined the soil suction consisted of three parts (Bridge and Willis, 2002):

- Suction mobilization: the suction force increasing from zero to maximum as the riser begins to move upwards;
- Suction plateau: the suction force remaining constant as the riser moves further upwards; and
- Suction release: the suction force decreasing from maximum with further upward movement of the riser to zero at the breakout displacement.

It was concluded that the soil suction force is independent of the consolidation time (Bridge and Willis, 2002). Willis and West (2001) back analyzed the experimental results using FEA programs such as Flexcom3-D, ABAQUS, and ANSYS, by defining specific contact elements that simulated the soil-riser interaction effects and the non-

linear and hysteretic force-distance curves, known as the “backbone curves”, that are associated with the interaction between a solid member and a clay soil. The numerical analyses performed satisfactorily in modeling the riser response when compared to the field data.

Complimentary to the STRIDE Phase 3 JIP was a series of small-scale laboratory SCR tests conducted under the Catenary Riser-Soil Interaction Model for Global Riser Analysis (CARISIMA) JIP. These tests were performed in two phases; Phase 1 (14 vertical and 17 horizontal tests) was completed during spring 2000, and Phase 2 (10 vertical and 6 irregular tests) was completed during spring 2001. The clay used in the experiments was taken from a reference site in Onsoy, located southeast of Norway. In the laboratory, the clay was consolidated under dead weight for a period of approximately six weeks. The test rig was originally designed to simulate the vertical (suction) and horizontal (pullout) motions of a SCR independently, however, in Phase 2 it was decided to modify the test setup to allow for simultaneous motion of the pipe sample both vertically and horizontally. The actuator design was capable of translating the SCR model ± 500 mm in the horizontal plane and ± 80 mm in the vertical plane. The main parameters monitored during execution of the tests (both vertically and horizontally) were loads, displacements, and accelerations (Sintef, 2001).

A numerical model was developed based on the CARISIMA test results (Bridge et al., 2004). For the vertical tests, one important observation made was that the

mobilized soil resistance was very dependent of the lift-off velocity. As part of the information/data exchange agreement between the CARISIMA JIP and the STRIDE Phase 3 JIP, full access to all test results provided further confidence in the CARISIMA numerical model through back-analysis of the STRIDE test results.

Bridge et al. (2004) developed an advanced analytical riser-soil interaction model based on the data obtained through the STRIDE and CARISIMA JIP's. The model consisted of two scenarios, with and without soil separation. Both scenarios were based on the backbone curve concept and considered soil suction forces and soil stiffness (i.e. static stiffness and small displacement dynamic stiffness) at various stages of the interaction. The models may be used to form the basis for numerical analysis, however, the authors stated that the dynamic soil stiffness models considered are conservative since they do not account for soil softening due to repetitive cycling and use bearing load as opposed to the touchdown point (TDP) reaction force for calculating soil stiffness.

The STRIDE and CARISIMA JIP's provided valuable insight in to the riser-soil interaction mechanism based on which, a number of analytical models were developed (e.g. Aubeny and Biscontin, 2009; Nakhaee and Zhang, 2010; Randolph and Quiggin, 2009). However, these JIP's simulated only certain aspects of the riser-soil interaction mechanism. For example, movement in the surge and sway directions (i.e. horizontal) were not simulated in the STRIDE program and the CARISIMA physical tests were mainly done with approximately 2 m straight section of 0.2 m diameter pipe.

Therefore, there is need to develop a tool that can correctly simulate as many aspects of the fluid-riser-soil interaction mechanism as possible. This is the main objective of the study presented herein.

3.4. MODELING CONSIDERATIONS

3.4.1. Motion Inputs and Need for a Cut-Off Model

Motions of semi-submersible vessels consist of high wave frequency and low natural vessel frequency components, which present the greatest challenge to the fatigue life of SCRs. Bhattacharyya et al. (2011) conducted a finite element analysis of a field SCR to evaluate whether the motions of a semi-submersible can be imposed on a sectional SCR (a section starting above the TDP and extending through the TDZ) for centrifuge modeling. The results indicated that properly scaled heave and surge motions can be applied at a hang-off point of a sectional SCR model in a centrifuge, and therefore is used as the main concept of this testing program. An overall schematic of a prototype SCR installation including the concept of the sectional SCR is shown in Figure 3-1; with positive heave upwards and positive surge away from the touchdown zone inducing tension onto to riser.

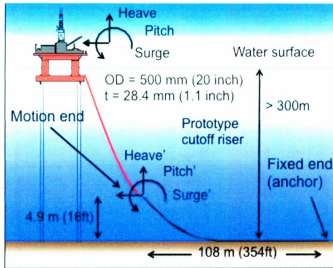


Figure 3-1: Schematic of prototype SCR with sectional SCR concept

To simulate the motions of a semi-submersible in the centrifuge, the actuation system required to be designed such that it was capable of simultaneously imposing a wide range of frequencies of heave and surge displacements on a sectional SCR model. To achieve this objective, consideration was given to design the actuation system for heave and surge motions with periods of 10 seconds and 200 seconds (in prototype terms), respectively, with a wide range of amplitudes. This was decided in consideration with the capacity of the servo-valves required. These periods may be slower (approximately four times) than those of actual storm events; however, the deformation and response of the seabed are of the main focus of the study and therefore, the compromise was made on the periods of

the motions as opposed to the amplitudes. The inertia effects of the slower motions on the soil in the centrifuge model are negligible.

Various field surveys and analysis indicate that the touchdown zone of a SCR is typically in the range of 110 m to 125 m. A 3.1 m long model box (see the following sections for further details) was fabricated to model an equivalent prototype 108 m section of a 0.5 m diameter SCR with a hang-off position approximately 4.9 m (16 ft) above the seabed. A challenge in the design of the model box was achieving a factor of safety of 1.25 to withstand the dynamic loading from the actuator, self-weight, and any other uncertainties.

3.4.2. Boundary Conditions

Only surge and heave motions were applied to the motion-end, with sway, yaw, and roll degrees of freedom fixed and the pitch degree of freedom treated as a hinged connection. Numerical models of the riser with and without pitch motion constraint concluded that the riser fatigue rates in both cases were similar in the touchdown zone and therefore, the hinged condition was considered adequate for SCR fatigue considerations.

Global riser model analysis indicated that the tension response of the riser resting on the seabed responds linearly to the axial motion of the cut-off point. An axial spring was therefore incorporated into the fixed-end of the model with the spring constant corresponding to the axial stiffness of the riser. The pitch rotation of the fixed-end was modeled as a hinged connection to help minimize the boundary effect in the touchdown zone. The hinged (pinned) connections were free of friction as practically as possible. A

ball-bearing system was used at the motion-end and lubricated shear-pin connection was used at the fixed-end.

Since the riser fatigue response is sensitive to tension, the initial tension in the model was controlled to match the global analysis results by adjusting the initial surge value at the motion end.

3.4.3. Capability for Riser-Fluid-Soil Interaction Modeling

Developing an actuation system that could closely simulate the scaled frequencies encountered in the field is important from two perspectives: 1) trench formation mechanism and, 2) the inertia effects in the riser. Erosion caused by the water velocity field generated from the motion of the riser plays an important role in the trench formation at the touchdown zone. This erosion is caused by the ambient fluid (mixture of the water and suspended soil particles eroded) shear stress imposed on the trench walls each time the riser departs and returns to the seabed. The magnitude of this shear stress varies along the touchdown zone. The interaction of the riser and soil with the ambient water is not fully understood and it is still a topic of further research.

The model tests were designed for fully submerged conditions. An attempt was made to develop an actuation system that could simulate as closely as possible the scaled frequencies typical of field conditions. However, the equipment limitations (hydraulic flow rates and valve requirements, etc.) allowed simulating motions that are about 2.3 to 4 times slower than those field equivalents. Analyses conducted by

Bhattacharyya et al. (2001) concluded that this limitation would have insignificant effect on the riser inertia. However, this limitation may cause the model scaling to be distorted with respect to soil erosion.

3.4.4. Centrifuge Scaling Considerations

Centrifuge experiments are ideally suited for modeling complex non-linear geotechnical problems where gravity is an important consideration. It is a well-established tool in geotechnical engineering in which the gravity in the model is increased by a factor N to produce an identical stress state to that in the prototype case. It is this factor N that is used to relate all other parameters of the model to prototype scale, summarized in Table 3-1. Fine-grained clay soil was used as the model seabed. Therefore, no scaling distortion exists with regards to particle size effects. The scaling distortion with regards to model velocity is described in Section 3.4.3.

Table 3-1: Scaling laws (after Taylor, 1995)

Parameter	Scale Factor
Length	$h_m = 1/N h_p$
Stress	$\sigma_m = \sigma_p$
Density	$\rho_m = \rho_p$
Acceleration	$a_m = N a_p$
Force	$F_m = 1/N^2 F_p$
Strain	$\epsilon_m = \epsilon_p$
Mass	$M_m = 1/N^3 M_p$

3.5. EXPERIMENTAL SETUP

Figure 3-2 illustrates the assembled package resting on the centrifuge basket prior to testing. The following sections describe the various components of the setup.

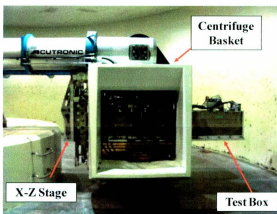


Figure 3-2: Centrifuge test setup

3.5.1. Test Box

The centrifuge has a payload surface area of 1,145 mm by 1,470 mm. To maximize the length of the model riser, the test box was extended beyond the limits of the centrifuge basket. The overall length of the test box was restricted to 3.1 m to prevent the box from contacting the central pedestal steps or the containment ceiling of the centrifuge during spin-up. The external width and height of the box were fixed at 250 mm and 500 mm to accommodate one riser and to provide adequate volume of clay for consolidation, respectively, while minimizing the overall payload mass. The internal dimensions of the box, therefore, were 3,049 mm long, 199 mm wide, and 475 mm high. Stress analyses were performed on the box design to verify the maximum overhang stress, bolt stress, and aerodynamic drag of the box were within the design criteria at 60 g.

The test box plates were fabricated from 25.4 mm (1") 6061 aluminum plates using an industrial water jet Computer Numerical Control (CNC) machine. The plates were assembled with an anaerobic gasket between contacting surfaces, and bolted together to create a watertight seal. The fully assembled test box was spun-up to 60 g in the centrifuge to verify design calculations and drag forces.

3.5.2. Motion Actuation System: X-Z Stage

The riser was controlled using a dual axis independently controlled hydraulic motion actuator, referred to as the X-Z stage, allowing the riser to be moved simultaneously in the vertical and horizontal planes (i.e. heave and surge). By resolving a desired two dimensional (2D) motion profile into heave and surge components and transmitting the drive signals to the X-Z stage actuator, an accurate reproduction of the motion could be physically produced and applied to the riser through a pin-connection between the truss members and motion-end clamp of the X-Z stage.

The X-Z stage was hydraulically controlled and therefore a specific position in X-Z space could be maintained for an extended time period. Electric servo motors could carry out the same mechanical function, but issues with holding currents at high loads and zero speeds, heat dissipation, and the use of electric braking systems could be problematic.

A balanced lifting force was required to solve two immediate issues. The first was the entire mass of the moving stage components including the surge system, riser model, and internal parts of the cylinder needed to be accounted for in the lifting force of the

cylinder. The second was that this force required to be applied evenly on both sides of the stage. Utilizing two cylinders to provide the balance lifting force would have required a large flow rate of oil and additional synchronization. The solution to these problems consisted of a set of force balancing cables and carefully positioned counterweights (Figure 3-3). This reduced the lifting capacity required by the cylinder, and removed the need for an additional cylinder to lift the system from both sides. The completion of the design consisted of carefully designed members that would carry the required load while minimizing the overall weight of the system, in addition to a guide roller and track system to maintain linear alignment of the system over the range of surge amplitudes. Aluminum was used extensively in the structure for minimizing the mass.

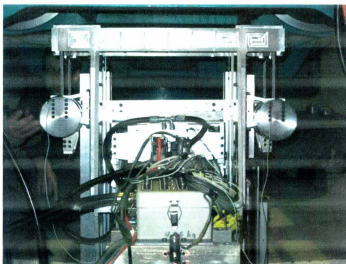


Figure 3-3: X-Z stage

The surge system design consisted of a separate structure complete with its own hydraulic cylinder and guide roller and track system. The selected cylinder was aluminum to minimize mass. Because this system operates in a plane normal to the direction of high gravitational force, no counter weight system was needed. The surge system was mounted to and moved with the heave system.

In addition to the hydraulic cylinders, servo valves, a manifold, and associated piping between components were required. Each servo valve spool was custom tailored for the calculated flow rate to generate the necessary velocities and accelerations required by the X-Z stage to produce the demanded motions.

Synchronization of the surge and heave axes was maintained using a unique control system comprising of two independent servo hydraulic control systems which simultaneously issue motion control data. The time step between successive motion command signals is sufficiently small enough to keep the two axes synchronized. A position error feedback loop was incorporated to stop the system if either axis fails to reach the command position.

The final design of the X-Z stage could operate at a maximum velocity of ± 200 mm/s with a maximum stroke of 340 mm in the vertical (heave) direction and at a maximum velocity of ± 35 mm/s with a maximum stroke of ± 15 mm in the horizontal (surge) direction.

Figure 3-4 illustrates a typical semi-submersible motion command and response of the X-Z stage. The actuator could hold the riser to ± 0.02 mm in heave and ± 0.002 mm in surge (Figure 3-5), with a 4 Hz dither in the surge signal caused by the hydraulic controller. The dual-frequency motion was typically a 1 Hz sine wave superimposed on a 0.05 Hz carrier sine wave (Figure 3-6).

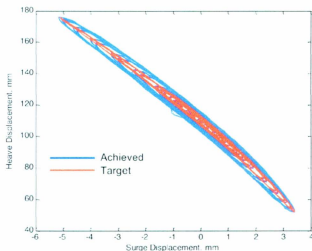


Figure 3-4: Typical riser motion

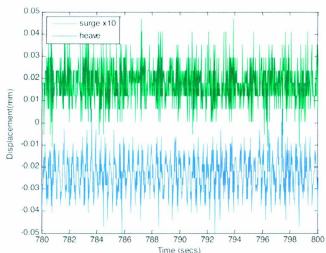


Figure 3-5: Holding accuracy of riser (Note: the surge displacement magnitudes have been exaggerated 10 times for clarity)

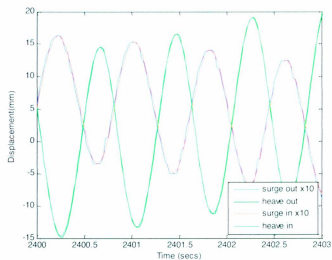


Figure 3-6: Sample of 1 Hz motions on 0.05 Hz carrier

3.5.3. Model SCR

The scale of the model riser was constrained by the maximum length of the test box that could be accommodated by the geotechnical centrifuge at C-CORE, and the minimum tubing diameter, which could be successfully strain gauged. The length of the model riser was therefore fixed at 2.8 m to maximize available room in the box and to allow space for the dual axis hydraulic control system (i.e. X-Z stage). Thin walled tubing of various materials and cross-sectional dimensions were investigated to find a suitable match to the desired prototype section modulus and submerged unit weight. Extruded 304 stainless steel seamless fractional stock tubing with an outside diameter of 12.7 mm and wall thickness of 0.711 mm matched a section modulus (Z) of $4.9E-3 \text{ m}^3$ in prototype terms. Comparing the outside diameter of the stainless steel tubing to the full-scale prototype riser (20 inch) gives a 40:1 scaled ratio. Thin-walled heat shrink was used to enclose the tubing to protect the instrumentation from the surrounding water during testing, but did not provide any structural capacity to the model. The heat shrink did, however, increase the overall diameter of the model from 12.7 mm to 14.1 mm. The total submerged weight of the model including the tubing and heat shrink, was too buoyant and required additional weight without increasing the bending stiffness. Small diameter PTFE (i.e. Teflon) balls were originally considered to fill the internal diameter of the tube to adjust the submerged weight; however, the PTFE balls restricted the riser and added to the riser bending stiffness. Ultimately, canola oil with a density of 920 kg/m^3 was used instead which resulted in a submerged weight of 67.3 N/m . Table 3-2 provides a complete summary of the riser model and equivalent prototype dimensions.

ASTM standard tensile tests were conducted on specimens of the original stainless steel tubing and determined that the tubing had an elastic modulus of 210 GPa and yield strength of 326 MPa at 0.01 % strain.

Table 3-2: Summary of riser model and equivalent prototype dimensions

Property	Model		Prototype	
	Value	Units	Value	Units
Outside diameter	12.7	mm	508	mm
Inside diameter	11.989	mm	479.6	mm
Wall thickness	0.711	mm	28.4	mm
Submerged unit weight	67.3	N/m	2.69	kN/m
Section modulus	76.04	mm ³	4.9E-3	m ³
Length	2.8	m	112	m
Pickup height	120	mm	4.8	m
Axial stiffness	881	N/mm	35.24	MN/m

3.5.4. End Conditions

The motion-end and fixed-end setups for the model riser are shown in Figure 3-7 and Figure 3-8, respectively. The conditions associated with the motion-end were described previously in Section 3.4.2. The fixed-end setup consisted of a pin connected joint that allowed the riser to freely rotate in pitch about its centerline and a vertical cantilever spring (i.e. upstand), fabricated from 4340 stainless steel, to provide an axial stiffness of 882 N/mm. The fixed-end setup was attached to the internal diameter of the riser tube using silver solder. Lab tests performed resulted in the tubing material failing prior to the soldered connection. The pin connected joint and upstand were attached to a linear guide block and rail that permitted the riser to transverse vertically, while preventing horizontal displacement. The guide block, clamping system, pin joint, and upstand were counterbalanced with a parallel system to remove the boundary affects created by these components.

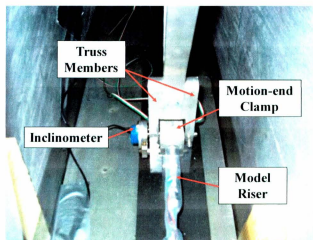


Figure 3-7: Motion-end of model SCR

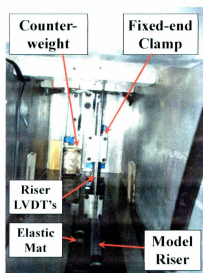


Figure 3-8: Fixed-end of model SCR

At the motion-end, the riser was connected to the hydraulic actuator system in which input motions were applied. A brass ring was silver soldered to the outside diameter of

the stainless steel tubing at a distance of 2,700 mm from the fixed-end pin connection. A clamp was designed to encompass the brass ring allowing tension to be applied to the riser without the clamp slipping over the tubing surface. Roller bearings were included in the motion-end clamp to create a pin connection between the riser and X-Z stage truss members and permitted the riser to rotate freely in pitch.

3.5.5. Instrumentation

Figure 3-9 shows the instrumentation layout for the model SCR. Full-bridge strain gauges were placed at 24 locations along the length of the riser tubing; 18 configured to measure bending moments concentrated around the estimated touchdown zone, three configured to measure axial tension at both the fixed and motion ends, and one bridge located on the upstand configured to measure tension through a cantilever design. The two remaining bridges were placed on the truss members of the X-Z stage in shear configuration to measure tension of the riser. Each bridge comprised of two 350 ohm gauge pair measuring 1.5 mm (0.06") long and 1.7 mm (0.065") wide with a polyimide backing 5.3 mm (0.21") long and 5.8 mm (0.23") wide. All strain gauges and wiring were completely enclosed in polyolefin thin-wall heat shrink tubing to protect against damage and water entry, except for the truss member strain gauges which were sealed and protected using Loctite 5900.

Table of Instrumentation

1	Inclinometer	- see detail A
2	LVDT#1 (elastic seabed)	- see detail B
3	Riser Strain Gauges	
4	PPTR1 (axial motion)	
5	PPTR2 (axial force)	
6	LVDT#2 (riser angle & settlement)	- see detail C
7	LVDT#3 (riser angle & settlement)	- see detail C
8	Laser # 1 (riser displacement)	
9	Laser # 2 (riser displacement)	

Notes:

- The strain gauge spacings are 100mm, 200mm & 300mm
- Test box inside dimensions: 3049.2 (L) x 199.2 (W) x 474.6 (H)
- All measurements are in millimeters

Table of Riser Strain Gauges

a	Axial	SG # 1	l	Bending	SG # 12
b	Bending	SG # 2	m	Bending	SG # 13
c	Bending	SG # 3	n	Bending	SG # 14
d	Bending	SG # 4	o	Bending	SG # 15
e	Bending	SG # 5	p	Bending	SG # 16
f	Bending	SG # 6	q	Bending	SG # 17
g	Bending	SG # 7	r	Bending	SG # 18
h	Bending	SG # 8	s	Bending	SG # 19
i	Bending	SG # 9	t	Axial	SG # 20
j	Bending	SG # 10	u	Bending	SG # 21
k	Bending	SG # 11	(upland)		

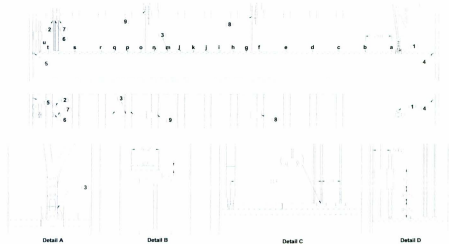


Figure 3-9: Instrumentation layout

The riser was also outfitted with two direct current (DC) precision linearly variable differential transformers (LVDTs) and two lasers. The LVDTs located 115 mm and 139 mm from the fixed-end separated from each other by a distance of 24 mm, were used to measure the vertical displacement of the riser and its rotation. The lasers (Figure 3-10), located 796 mm and 1,606 mm from the fixed-end, measured the displacement of the riser by measuring the displacement of a plate and rail system attached to the riser using thin nylon rope. As the riser was lifted vertically, the plate moved downwards.

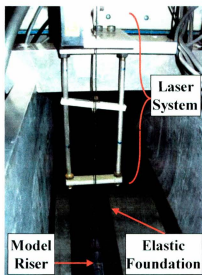


Figure 3-10: Laser system and model SCR on elastic seabed

Attached to the motion-end clamp and test box were miniature liquid capacitive inclinometer sensors used to measure the rotation of the riser and test box. Since the shear gauges located on the truss members only respond to loads applied in the horizontal (surge) direction, the inclination of the riser at the motion-end was required to calculate the resultant tension of the riser. The X-Z stage was instrumented with a 355.6 mm (14") Honeywell Longfellow II linear position transducer (LDT) and an LVDT to measure the displacement of the motion-end clamp in the vertical (heave) and longitudinal (surge) directions, which correspond to the riser motions. The X-Z stage was also outfitted with two accelerometers to measure the acceleration in the heave and surge directions.

3.6. ELASTIC SEABED TEST RESULTS

The model SCR and actuation system were tested at 40 g with the riser resting on an elastic bed material comprised of closed cell neoprene with an elastic modulus of 159 kPa. The objectives of these tests were:

- To evaluate the performance of the test package as a whole under 40 g;
- To evaluate the accuracy, control, and response of the X-Z stage and the instrumentation system; and
- To investigate the capability of the model SCR in capturing the catenary deformation under various boundary conditions (i.e. tension and deformation values).

The motion-end of the SCR was initially lifted to a height of 120 mm above the seabed. The riser was then tensioned to an initial pre-determined tension magnitude by adjusting the surge displacement of the X-Z stage. The riser was then displaced ± 20 mm incrementally in heave direction without adjusting the surge. This procedure was performed for three initial tensions, 375 N, 365 N, and 400 N. A summary of the heave response of the X-Z stage is shown in Figure 3-11. Bending moment profiles of the riser for test tensions 401.1 N, 660.6 N, and 90.7 N are summarized in Figure 3-12, Figure 3-13, and Figure 3-14, respectively. SG14 and SG19 were unresponsive during the centrifuge test and thus are not shown.

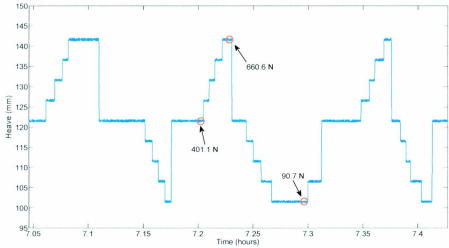


Figure 3-11: Heave input with corresponding tension values

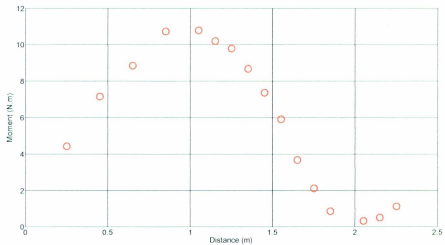


Figure 3-12: Bending moment profile for 401.1 N tension

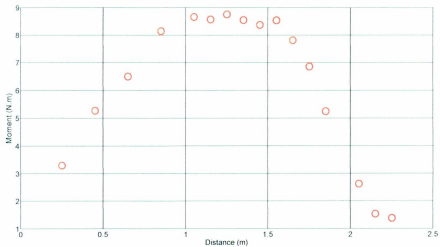


Figure 3-13: Bending moment profile for 660.6 N tension

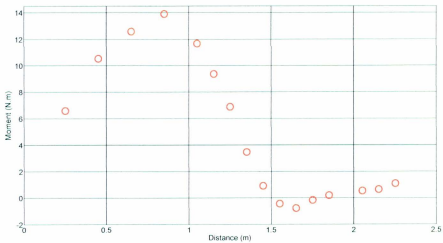


Figure 3-14: Bending moment profile for 90.7 N tension

3.7. NUMERICAL MODEL OF ELASTIC SEABED TEST

The riser and elastic seabed were modeled using the finite element software package ABAQUS as a two dimensional interaction. The objectives were to evaluate the overall performance of the elastic seabed test, validate the scaling of the model, and identify and quantify the friction between the elastic seabed and riser and any other deficiencies in the system.

The riser itself was modeled using linear beam elements (B21) with a cross-section having an outside diameter and wall thickness of 12.7 mm and 0.71 mm, respectively. The weight of the heat shrink and oil within the riser were accounted for by adding mass elements along the riser, which added no structural capacity to the system. Buoyancy and surface interactions were calculated based on an effective outside diameter of 14.1 mm (i.e. outside diameter of riser plus thickness of heat shrink). The numerical riser was assumed to be elastic with a total submerged weight of 67.3 N/m at 40 g.

The upstand was included in the FE model with a pin connection between the upstand and the riser to incorporate the fixed-end condition. The upstand was modeled as a solid circular section measuring 11 mm in diameter and having the same material properties as the riser. The upstand was free to displace in the vertical (heave) direction to follow settlement of the elastic seabed during spin-up; however, it was restricted from moving in the horizontal direction (surge) and restricted from rotating about the yaw axis.

The elastic seabed was modeled as a 2D analytical rigid shell with surface-to-surface contact. The normal behaviour of the seabed was defined by 1.9 times the elastic modulus of neoprene established from a physical test performed in the laboratory. This discrepancy was a result of the change in elastic behaviour of the neoprene under 40 g. The contact model provided continuously interaction behaviour along the length of the riser between the riser and elastic seabed as compared to the discrete spring model. Surface friction was added using a friction coefficient of equal to 0.4.

Input motions were included in the numerical analyses with the specified three initial tensions. At a first glance, the results from the numerical model reasonably yielded the same bending moment profiles as the physical test. Small discrepancies were observed at the motion-end, fixed-end, and touchdown zone. Further investigations into the physical test indicated that there was a 3 N.m moment about the yaw axis at the motion-end as a result of a slight misalignment between the motion-end clamp and truss members. This was incorporated into the numerical model as a constant 3 N.m moment at the motion-end clamp; however, in the physical test this moment varied depending on the riser orientation and tension.

The bending moment profile of the physical test initially indicated that there was an increase in moment approaching the fixed-end, which was not observed in the numerical model. Further investigation deduced by weighing the upstand components and counter weight designed to balance the upstand in the physical test indicated that the counter

weight required to be 40 grams lighter. This resulted in an upward applied force to the upstand of 15.7 N. Figure 3-15, Figure 3-16, and Figure 3-17 compare the results from the FE model and centrifuge test for tensions 401.1 N, 660.6 N, and 90.7 N after applied appropriate corrections, respectively.

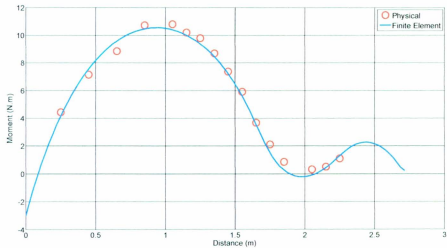


Figure 3-15: Comparison of physical and FEA for 401.1 N tension

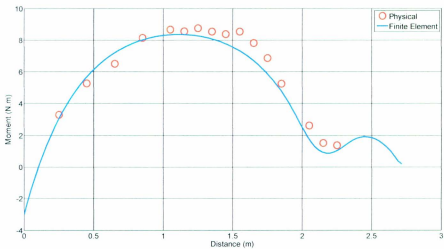


Figure 3-16: Comparison of physical and FEA for 660.6 N tension

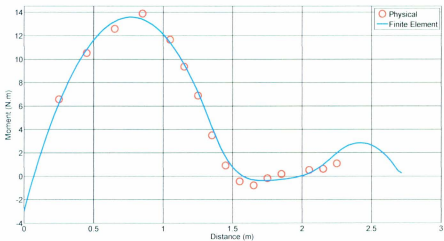


Figure 3-17: Comparison of physical and FEA for 90.7 N tension

3.8. CONCLUSIONS

A novel experimental apparatus was developed and successfully tested for simulating an SCR at the touchdown zone. The apparatus was capable of simulating Response-Amplitude-Operator (RAO) motions of a semi-submersible vessel in a two-dimensional plane for wide range of frequencies while applying an appropriate tension to the riser. Through the elastic seabed tests and complementary FEA modeling, it was demonstrated that centrifuge scaling laws can be successfully applied to simulate a complex engineering phenomenon such as interaction of a SCR with the ambient fluid and seabed. Step-by-step scaling and development procedures have been explained. Both the centrifuge and FEA models provided the bending moment profile along the length of the SCR for a range of tension magnitudes. These models could therefore be further advanced to include a non-elastic seabed (i.e. physical soil) in which fatigue analysis and trench formation could be studied. These aspects of the SCR-soil interaction were the focus of Part II of this research program.

3.9. ACKNOWLEDGEMENTS

This work was supported by C-CORE. We would like to thank C-CORE staff, in particular, John Barrett, Don Cameron, Derry Nicholl, and Karl Tuff for their help in the development and execution of the centrifuge tests.

3.10. REFERENCES

Aubeny, C. P., and Biscontin, G., 2009. "Seafloor-Riser Interaction Model," *International Journal of Geomechanics* 9(3), pp. 133-141.

- Bhattacharyya, A., Tognarelli, M. A., Li, G., Ghosh, R., Clukey, E. C., and Sun, Q., 2011, "Simulation of SCR Behavior at Touchdown Zone - Part I: Numerical Analysis of Global SCR Model vs. Sectional SCR Model." Offshore Technology Conference, OTC 22557, Rio de Janeiro, Brazil, pp. 1-10.
- Bridge, C., Howells, H., Toy, N., Parke, G., and Woods, R., 2003, "Full Scale Model Tests of a Steel Catenary Riser," International Conference on Fluid Structure Interaction, Cadiz, Spain, 10p.
- Bridge, C., Laver, K., Clukey, E., and Evans, T., 2004, "Steel Catenary Riser Touchdown Point Vertical Interaction Models," Offshore Technology Conference (OTC) 16628, Houston, Texas, USA, pp. 1-9.
- Bridge, C., Willis, N., 2002, "Steel Catenary Risers – Results and Conclusions from Large Scale Simulations of Seabed Interaction," Proceedings of the International Conference on Deep Offshore Technology, New Orleans, Louisiana, USA, 15p.
- Nakhaee, A., and Zhang, J., 2010, "Trenching Effects on Dynamic Behavior of a Steel Catenary Riser," Ocean Engineering, 37(2-3), pp. 277-288.
- Randolph, M., and Quiggin, P., 2009, "Non-linear Hysteretic Seabed Model for Catenary Pipeline Contact," Proceedings of the ASME 2009 28th International Conference on Ocean, Offshore and Arctic Engineering, OMAE2009-79259 Honolulu, Hawaii, USA, pp. 1-9.
- Sintef, M., 2001, "The CARISMA JIP: Catenary Riser/Soil Interaction Model for Global Riser Analysis (CARISIMA) ",

Taylor, R.N., 1995. "Geotechnical Centrifuge Technology". Blackie Academic & Professional, London.

Willis, N. R. T., West, P. T. J., 2001, "Interaction between Deepwater Catenary Risers and a Soft Seabed: Large Scale Sea Trials," OTC 13113, Offshore Technology Conference Houston, Texas, April 30–May 3, 9p.

**4. CENTRIFUGE MODELING OF STEEL CATENARY RISERS AT
TOUCHDOWN ZONE PART II: ASSESSMENT OF CENTRIFUGE TEST
RESULTS USING KAOLIN CLAY**

Submitted to: Ocean Engineering, Date of submission: March 30, 2012.

*Authors: Bradley J. Elliott, Arash Zakeri, John Barrett, Bipul Hawlader,
George Li, Edward C. Clukey.*

4.1. ABSTRACT

This paper presents the results of an experimental investigation into the fatigue issues related to steel catenary risers (SCRs) within the Touchdown Zone (TDZ). The experiment was conducted in the C-CORE geotechnical centrifuge using the apparatus described in Part I (the companion paper). Kaolin clay with an undrained shear strength profile typical of deepwater Gulf of Mexico was used for the model seabed. The model riser simulated an approximately 108 m long, 0.5 m diameter SCR subjected to four sets of synthetic heave and surge motions ranging in complexity from a simple sinusoidal wave to those having characteristics of dual frequency Response-Amplitude-Operator (RAO) motions. The results provided valuable insights into the fluid-riser-soil interaction mechanism, trench formation and its influence on the fatigue stresses of an SCR. The results indicated that the trench geometry had a significant influence on the fatigue stresses. The formation of the trench in this experimental program resulted in considerable reduction (as high as about 20%) in bending and tensile fatigue stresses. The experimental program demonstrated that the fatigue life of an SCR could potentially increase as the trench developed from its original mudline state.

4.2. INTRODUCTION

This paper presents the results of a series of experiments conducted in a geotechnical centrifuge as part of a large research program aiming to investigate fatigue damage on a Steel Catenary Riser (SCR) within the Touchdown Zone (TDZ). The overall objectives of the program was to develop a testing apparatus to simulate a SCR within the TDZ subjected to various motions representative of those induced by a floating platform in storm conditions, to understand the fluid-riser-soil interaction mechanism, and to investigate the influence of the resulting trench on the fatigue life of the riser. The results of this research program are summarized in two papers. Part I (Elliott et al., (submitted March 2012)) describes the development of the testing apparatus, scaling of the experiments, and the procedures for the validation of the model riser on an elastic seabed and the associated Finite Element Analysis (FEA). This paper, Part II, describes preparation of the model seabed, the riser motions and testing procedures, and test results. All results herein are presented in model terms unless otherwise noted. Most figures present the results in both model and prototype terms. The scaling laws and conversions are provided in Part I.

4.3. PHYSICAL SETUP AND DESIGN PARAMETERS

4.3.1. Model Riser Properties and Boundary Conditions

The riser geometry and material properties remained unchanged from the elastic seabed test described in (Elliott et al., (submitted March 2012)). The model riser was made of commercially available stainless steel tubing, with an outside diameter of 12.7 mm and a

wall thickness of 0.711 mm (508 mm and 28.4 mm, respectively, in prototype terms). It was instrumented with strain gauges, filled with canola oil (to achieve the targeted submerged unit weight), and encased with a heat shrink to protect the underlying strain gauges. The instrumented model riser with the heat shrink had an outside diameter of 14.1 mm and a submerged unit weight of 67.3 N/m (2.69 kN/m in prototype terms). The modulus of elasticity of the riser was determined to be 210 GPa through the use of ASTM standard tensile tests.

4.3.2. Riser Boundary Conditions

A pin and roller bearing connected the motion-end of the riser to the X-Z stage to allow it to freely rotate in pitch, the axis normal to the plane of the applied heave and surge motions. At the fixed-end, the riser was connected to an upstand attached to the test box with a clamp and counterweighted linear guide block system. The fixed-end was free to translate vertically, following consolidation and self-trenching deformations, and to rotate in pitch about the axis normal to the plane of the heave and surge motions. The height of the upstand was adjusted to achieve an axial stiffness of 881 N/mm (35.24 MN/m in prototype terms) in the riser.

4.3.3. Model Seabed Preparation and Properties

Kaolin clay was used to make the model seabed. The clay was reconstituted from slurry with a moisture content of 120 % (twice the liquid limit), and consolidated to a final depth of 77 mm under a final vertical effective stress of 55 kPa to achieve the target undrained shear strength of that shown in Figure 4-5. The target strength profile

consisted of 4 kPa crust to about 600 to 800 mm depth (15 to 20 mm in model scale) increasing at a rate of 1.6 kPa/m below the crust. This profile was thought to be representative of deepwater conditions in the Gulf of Mexico and was similar to conditions used by others in SCR studies (Aubeny and Biscontin, 2009).

4.3.4. Applied Motions

Four sets of artificial motions were applied to the model riser to investigate the trench formation mechanisms (such as erosion and rate effects) and the influence of trench depths on fatigue stresses. Each motion had a different amplitude and frequency and was applied in the heave and surge directions, illustrated on Figure 4-1 in model terms. For all motions, the heave to surge ratio was fixed at 14 and positive surge induced tension in riser (i.e. away from the fixed-end) and positive heave resulted in displacement up and away from seabed. The first motion (M1) consisted of a simple sinusoidal function with heave and surge amplitudes of 30.0 mm and 2.11 mm, respectively, both having a frequency of 0.05 Hz. The second motion (M2) was developed to include a higher superimposed secondary frequency in the applied motion without increasing the overall amplitude.

To obtain a more representative riser motion in the TDZ of the model, a simple oscillating wave motion was translated along the length of the riser from the water surface to 4.9 m above the seabed, in prototype scale. This created a complex dual frequency waveform, shown in Figure 4-1 (c) and (d) in model scale, with frequencies of 0.05 Hz and 1 Hz. The heave and surge neutral axes were shifted upwards by 2.89 mm

and the surge was phased shifted by 0.26 seconds from the heave motion, shown by the separation from the linear line in Figure 4-2. The fourth motion (M4) increased the magnitudes of the surge and heave displacements of M3 by 50 % without changing the frequencies or phase shifts. M3 and M4 are motions characteristic of a riser induced by a floating platform in storm conditions, however, are purely artificial and do not represent any specific geographic location.

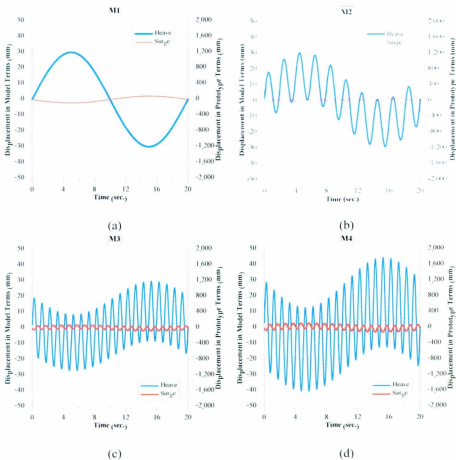


Figure 4-1: Motions used in centrifuge test: M1 (a), M2 (b), M3 (c), and M4 (d)

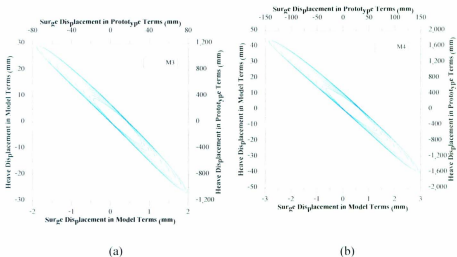


Figure 4-2: Heave versus surge displacements: M3 motion (a) and M4 motion (b)

4.3.5. Instrumentation

Figure 4-3 presents the instrumentation layout of the model riser and the clay seabed. A complete description of all instruments used during the test series are provided in Sections 4.3.6 to 4.3.9.

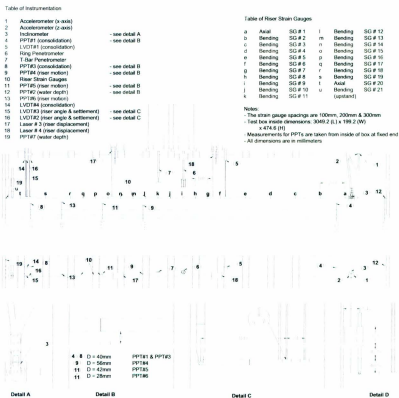


Figure 4-3: Instrumentation layout with clay bed

4.3.6. Pore Pressure Transducer

Seven miniature Pore Pressure Transducers (PPTs) were used. Two PPTs were installed on the surface of the clay to measure the height of the free surface water, two PPTs were installed at approximately half the clay depth to measure the dissipation of excess pore pressures during consolidation, and four PPTs were installed in close proximity to the riser at depths of two, three, and four times the riser diameter.

4.3.7. Displacement Measurements

In addition to the PPTs installed in the clay, consolidation was also monitored using two Linear Variable Differential Transformers (LVDTs) on the clay surface at opposite ends of the test box. Two additional LVDTs were mounted on the riser at the fixed-end using extension rods with semi-circular cradles, separated by a distance of 24 mm. This allowed for both the settlement and inclination of the riser at the fixed-end to be measured. Lasers were also used to measure the settlement and displacement of the riser at 0.8 m (Laser 1) and 1.6 m (Laser 2) from the fixed-end. Each laser system consisted of a small freely sliding plate that was connected to the riser with a string and pulley. The laser beam reflected from the plate and allowed measurement of the riser and trench deformations during the tests.

4.3.8. Inclinometers

Two inclinometers were used during these tests, one attached to the test box to measure the rotation of the centrifuge swing, and a second attached to the motion-end clamp to measure the inclination of the riser at the pickup point.

4.3.9. Riser

The riser was instrumented with 22 full bridge strain gauge pairs; 18 oriented to measure the bending response of the riser, and three to measure the riser tension (strain gauge 21 (SG21) at the fixed-end and SG1 and SG1b at the motion-end). Two additional full bridge pairs were installed on the truss members, connecting the riser to the X-Z stage. These gauges measured the horizontal component of the riser tension and the resultant

tension was calculated by the truss response corrected by using the inclination measured by the inclinometer attached to the motion-end clamp. The locations of the strain gauges along the length of the riser are tabulated in Table 4-1.

Table 4-1: Riser strain gauge locations

Strain Gauge	Measurement	Distance from Motion pin (mm)	Strain Gauge	Measurement	Distance from Motion pin (mm)
Truss	Tension	0	SG # 11	Bending	1651.5
SG # 1	Tension	51.5	SG # 12	Bending	1751.5
SG # 1b	Tension	201.5	SG # 13	Bending	1851.5
SG # 2	Bending	351.5	SG # 14	Bending	1951.5
SG # 3	Bending	551.5	SG # 15	Bending	2051.5
SG # 4	Bending	751.5	SG # 16	Bending	2151.5
SG # 5	Bending	951.5	SG # 17	Bending	2251.5
SG # 6	Bending	1151.5	SG # 18	Bending	2351.5
SG # 7	Bending	1251.5	SG # 19	Bending	2451.5
SG # 8	Bending	1351.5	SG # 20	Tension	2651.5
SG # 9	Bending	1451.5	SG # 21	Tension	2716.6
SG # 10	Bending	1551.5			

4.4. PROCEDURES FOR CENTRIFUGE TESTS

The following is a summary of all the test procedures developed by C-CORE for this centrifuge testing program, including setup, consolidation, lifting and lowering of the riser, application of motions, and soil characterization tests.

4.4.1. Consolidation Phase

- Start data acquisition sampling at a rate of 1 Hz with a signal conditioning filter of 100 Hz.

- Spin centrifuge up to test speed (40 g). Monitor riser tension and adjust accordingly to maintain a tension of approximately 100 N.
- Monitor PPTs installed in the clay for dissipation of excess pore pressure, and LVDTs for surface settlement until 95 % consolidation is achieved; verified by using the root time method.

4.4.2. Applied Motions

- Lift the riser until the centerline is 120 mm above the clay surface at the motion-end while maintaining a tension of approximately 100 N.
- Tension riser to the target tension (350 N) at the motion-end by adjusting the surge axis of the X-Z stage.
- Increase the data acquisition sampling rate to 40 Hz with a signal conditioning filter of 100 Hz.
- Apply the motions in packets, each packet having 20 cycles, separated by period of 30 seconds. The sequence of motions is summarized in Table 4-2. Also, see Figure 4-1, Figure 4-2, and Figure 4-4 for further details of the applied motions.

Table 4-2: Testing sequence

Motion	Packets	Cycles	Duration (min)
M1	3	60	20
M2	3	60	20
M3	3	60	20
M4	3	60	20
M2	3	60	20

- Lower riser until the centerline of the riser is 13 mm above the clay surface at the motion-end while maintaining a tension of approximately 100 N.

4.4.3. Soil Characterization Tests

- Activate the T-bar vertical drive at 3 mm/s to obtain the clay strength profile.
- Cycle the T-bar up / down (10 cycles) to measure the remoulded strength profile of the clay.
- Activate the ring penetrometer vertical drive at 10 mm/s to obtain the clay strength profile.
- Cycle the ring penetrometer up / down (10 cycles) to measure the remoulded strength of the clay.

4.4.4. End of Test / Post Test Measurements

- Centrifuge stop – spin down to 1 g.
- Core samples of the clay were taken at opposite ends of the test box and measured for moisture content per 10 mm depth increments.
- The clay was digitized using a coordinate measuring machine (CMM).

4.5. TEST RESULTS AND DISCUSSION

4.5.1. Heave and Surge Motions

Following completion of the in-flight consolidation, the riser was lifted to 120 mm above the seabed, equivalent to 4.9 m in prototype terms, and tensioned to approximately 350 N. After tensioning riser, the surge and heave motions were applied. Figure 4-4

illustrates the motions applied and their sequences. Each packet contained 20 cycles and was separated by a 30 second interval to allow for excess pore pressures to dissipate.

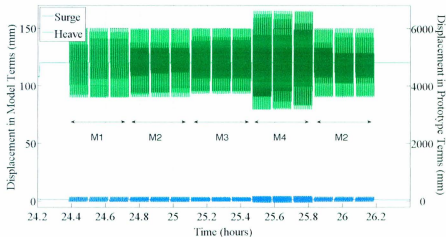


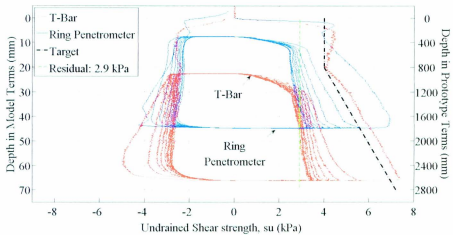
Figure 4-4: Applied motions

4.5.2. Shear Strength of Model Seabed

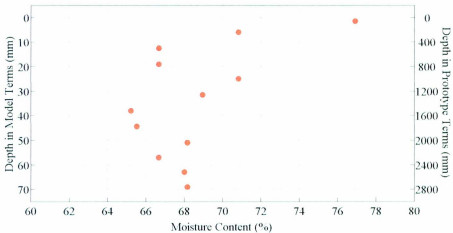
The clay consolidated under 40 g for a period of 2.7 hours reaching 95 % consolidation at 1.83 hours with an overall settlement of 1.2 mm. 95 % consolidation was chosen to ensure almost no excess pore pressure exist prior to applying the motions. The water level above the clay and the excess pore pressures were also monitored. The undrained shear strengths (s_u) was measured in-flight at two locations using a miniature T-bar and a ring penetrometer. The T-bar was 8 mm in diameter and 30 mm in length. The ring penetrometer, developed at C-CORE, consisted of a 2.4 mm diameter stainless steel wire formed into a 35 mm diameter ring. It had the same operational principles as the T-bar, with the advantage of being able to measure s_u at shallower depths. The T-bar and ring

penetrometer were inserted into the clay at rates equal to 3 mm/s and 10 mm/s, respectively, calculated based on the recommendations made by Finnie and Randolph (1994). It should be noted that rate effects are important and required to be considered. For example, an increase by a factor of just over 10 would be expected to give strengths some 20 % higher (e.g. Lehane et al., 2009).

The measured and targeted s_u and moisture content profiles are shown on Figure 4-5 (a) and (b), respectively. The clay had an average residual shear strength of 2.9 kPa and an average moisture content of 69 %. The ring penetrometer measured slightly higher shear strengths below 10 mm depth, due to the design and location of the load cell. The T-bar load cell was located immediately above the cross bar and measured only the resistance created by the flow of clay around the bar, whereas the ring penetrometer load cell was located on a cruciform connected to the ring by three 2.4 mm diameter rods and was affected by the resistance of the rods as they passed through the clay. It should be noted that the ring penetrometer was designed to measure s_u within the upper 10 mm only.



(a)



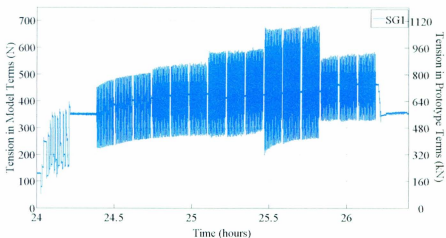
(b)

Figure 4-5: Undrained shear strength (a) and water content (b) profiles in model terms

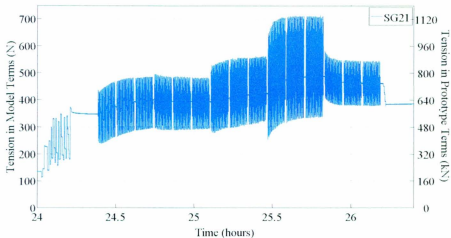
(note: zero on the y-axis corresponds to mudline)

4.5.3. Tension Forces

Figure 4-6 presents the tensions measured by SG 1 and SG 21 (see Figure 4-3 for location) at the motion-end and fixed-end, respectively. The tension forces at the fixed-end were lower than those measured at the motion-end because of the catenary action and partly due to the axial friction in the trench and surface zone. During the M1 and M2 motions, there was an increase in the tensions as the trench was formed and as its depth increased with time. The overall amplitude of the M3 motion was slightly smaller than those of the M1 and M2 in the downward direction, however, the out-of-phased surge created higher tensions in the riser. Further, the increase in tension measured by SG21 suggested that the trench geometry changed and the deepest point shifted towards the fixed-end during the M3 motion. The M4 motion had the largest overall amplitude, which was reflected in the tension measured as the trench increased in depth. The tension magnitudes dropped and remained constant during the last M2 motion, which indicated that the trench had reached a steady-state condition and its geometry did not change significantly.



(a)

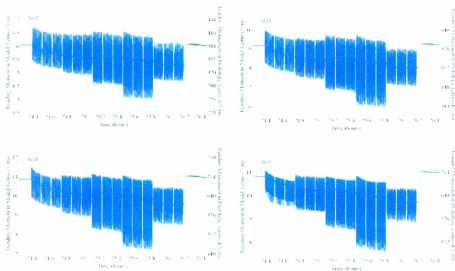


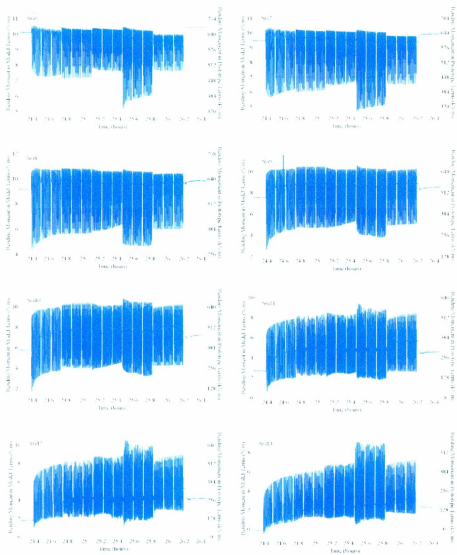
(b)

Figure 4-6: Tension of SG1 (a) and SG21 (b) during applied motions. From the left, each three sets represent M1, M2, M3, M4 and M2 motions, respectively.

4.5.4. Bending Moments

Figure 4-7 (see page 4-20 for figure caption) shows the bending moments measured by the strain gauges in model terms. SG14 and SG19 were unresponsive during the centrifuge test and thus are not shown. Figure 4-8 presents the bending moment profiles taken before and after implementation of each series of motions. The influence of trench formation and increase in trench depth as the motions were applied are evident from this figure. The magnitude of the bending moments decreased as the trench depth increased (see Section 4.5.5 for trench data) and with this, the point of maximum moment shifted towards the fixed-end. The two kinks in the bending moment profiles near SG8 and SG12 were caused by the strings attached to the riser as part of the laser measuring system (Figure 4-8), which applied a nominal point load of 2.1 N.





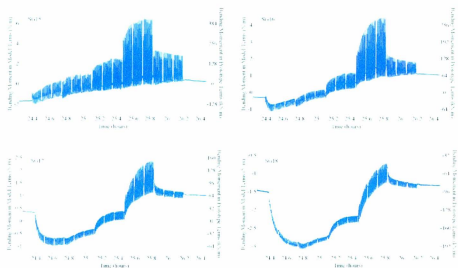


Figure 4-7: Response of bending strain gauges (note: scale of Y axes may be different).
 From the left, each three sets represent M1, M2, M3, M4 and M2 motions, respectively.

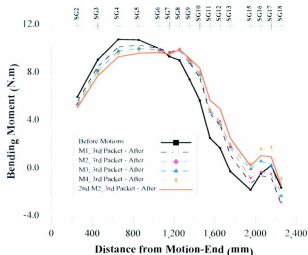
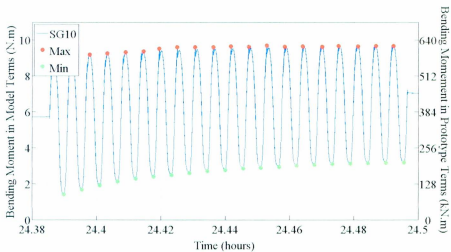
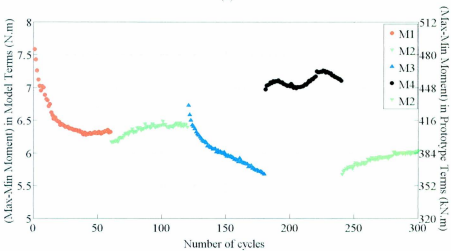


Figure 4-8: Bending moment profiles before and after motions

Strain gauges SG9, SG10, and SG11 measured the largest peak-to-trough magnitudes of bending moments, which correspond to a zone where fatigue damage would be most significant (discussed in Section 4.5.8). Figure 4-9 (a) presents the bending moments measured in SG10 during the M1 motion. Figure 4-9 (b) shows the difference between the consecutive maximum and minimum values (peaks and troughs) measured during all the motions for SG10.



(a)



(b)

Figure 4-9: Bending moments measured by SG10 during M1 motion (a), and SG10 bending moment difference between consecutive maxima and minima versus number of cycles in all motions (b)

4.5.5. Trench Data

Figure 4-10 shows the measurements made by Lasers 1 and 2. Each laser applied a nominal load of 2.1 N at the point of connection to the riser. The sinusoidal M1 motion formed the initial trench. The M2 motion was a combination of two sine functions with in-phased heave and surge; however, it did not represent realistic storm characteristics and was only applied to investigate erosion caused by agitating the water in vicinity of the riser. The amplitude of the M2 motion was the same as M1 but contained a higher frequency component. This secondary frequency did not have a significant influence on the trench formation. The M3 motion increased the depth of the trench despite having slightly smaller overall amplitude in the downward direction than the M1 and M2 motions. The M4 motion, the largest motion, increased the depth of the trench and reached steady-state condition towards the end.

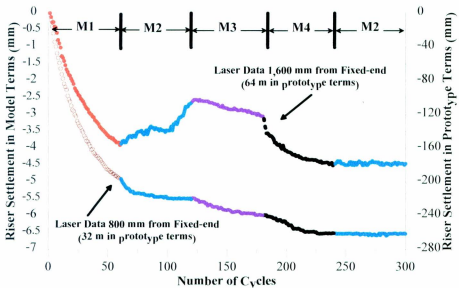


Figure 4-10: Laser measurements versus number of applied cycles

Upon completion of the test, excess water was removed from the clay surface and the final trench and berm geometries were digitally scanned using a coordinate measuring machine (CMM). Figure 4-11 and Figure 4-12 show the three-dimensional and plan views of the final trench and berm geometries as measured by the CMM. The color bars shown in the figures indicate depth in mm.

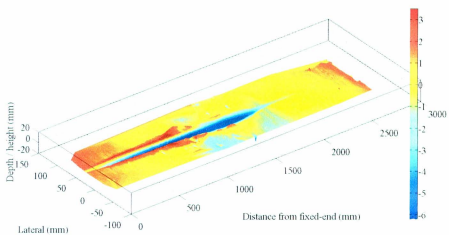


Figure 4-11: Three-dimensional view of the final trench geometry (color bar indicate depth in mm)

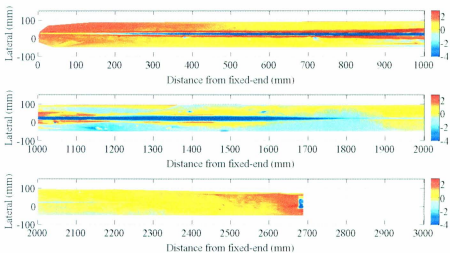


Figure 4-12: Plan views of final trench geometry. Zero corresponds to the fixed-end.

Lasers were located 800 mm and 1,600 mm from the fixed-end. The legend is in model terms. For conversion one needs to multiply by 40.

Figure 4-13 presents the mudline, trench, and berm geometries. At its greatest depth, the trench was approximately equal to the diameter of the riser. ROV field observations show that the trench could be as deep as three to four times the riser diameter. It is likely that the erosion caused by the water velocity field around the riser plays a significant role in the trench formation mechanism. It appears this erosion aspect was not fully captured in this test, and therefore, it is postulated that this aspect of the fluid-riser-soil interaction was not properly scaled in the current centrifuge test setup.

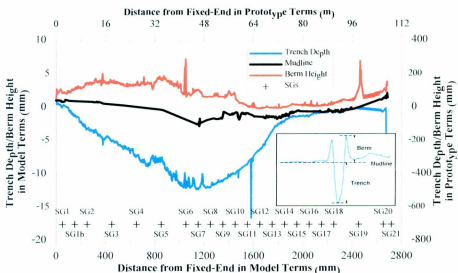
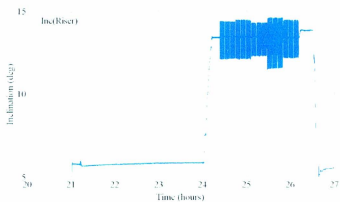


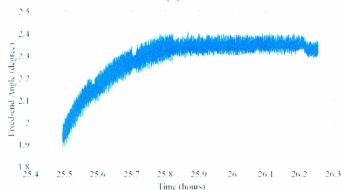
Figure 4-13: Final trench base and berm height profiles

4.5.6. Riser Inclination at Boundaries

Figure 4-14 presents the inclinations at the motion-end (a) and fixed-end (b). The fixed-end of the riser was slightly affected by the M4 motion as its slope changed from about 1.9 degrees to 2.4 degrees. This change was insignificant and the system performed well. The motion-end rotated approximately 7.5 degrees as the riser was lifted to 120 mm above the seabed, with an average rotation of approximately ± 1 degree during the applied motions.



(a)



(b)

Figure 4-14: Riser inclination data at the motion-end with positive showing clockwise rotation (a) and at the fixed-end (b)

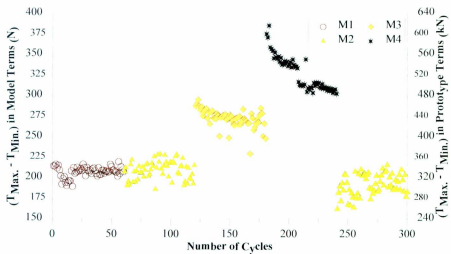
4.5.7. Pore Pressures

The water level was monitored and maintained using the surface PPTs located at each end of the test box. The riser was fully submerged throughout the test. PPTs 4, 5, and 6 were placed at 28 mm, 42 mm, and 56 mm depth, respectively, in close proximity to the

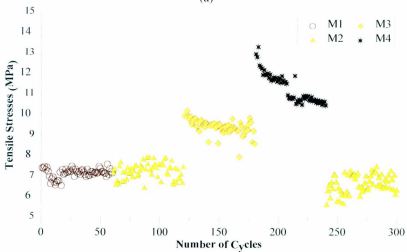
riser to measure the pore pressure response in the clay during the motions. The motions produced nominal excess pore pressures that dissipated quickly after termination of the motion packets.

4.5.8. Fatigue Stresses

Figure 4-15 plots the difference between the maxima and minima (peaks and troughs) in the tension measures at the motion-end by SG1. Despite the increase in overall magnitudes of the tension, the difference between the maximum and minimum values measured remained rather constant during the simple sinusoidal motion of M1. Introduction of a second component to the motion caused some scatter in the difference between maxima and minima as observed during application of M2 with the moving average being the same as that of M1. Interesting to note was the decrease in the magnitude of the difference between maxima and minima tensions during the M3 and M4 motions, which have the RAO characteristics. This decrease was about 7 % for the M3 motion and approximately 18 % for the M4 motion from commencement. Fatigue from only axial stresses was less of a concern in design of SCRs, however; one needs to consider axial stresses in combination with bending stresses. Fatigue life is a non-linear function in conjunction with these stresses and on a percentage basis will be much higher by a power of somewhere between three and five of the stress level.



(a)



(b)

Figure 4-15: Difference between maxima and minima tensions in SG1 versus number of cycles (a) and tensile stresses versus number of cycles (b)

Figure 4-16 shows the difference between the maxima and minima bending stresses (essentially the fatigue stresses, but these levels require to be factored by power of 3 to 5 for fatigue life) in SG10 against the numbers of cycles in all motions. Of significant importance was the approximate 20 % reduction in the fatigue stresses during the M1 and M3 motions. Both series of M2 motion produced a sparse range of tensions and a slight increase in the fatigue bending stresses of similar characteristics.

The M4 motion was the largest and therefore, produced the largest fatigue stresses in riser and deepened the trench. Although in terms of the bending stresses it did not show the same trend as the M3, the influence of trench is evident in the tensile stresses. However, the ratio of the stress difference for M4 to stress difference at the end of M3 is less than about 1.25 given that the amplitudes of M4 was 1.5 of those of M3. This also indicates the effect of trench depth in increasing the fatigue life has already taken place. Comparison of the results from the two M2 motions seems to support this argument.

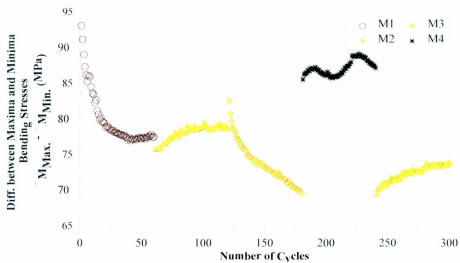


Figure 4-16: Difference between consecutive maxima and minima bending stresses in SG10 versus number of applied cycles

4.6. CONCLUSIONS

The experimental setup performed very satisfactorily. The test provided valuable insights into various aspects of the fatigue issues related to the SCRs near the touchdown zone. These included trench formation mechanism and its influence on the fatigue life, the fluid-riser-soil interaction mechanism, and pore pressure generated in the vicinity of the riser. It was believed the current setup, however, did not fully model the erosive mechanism of the water velocity field on seabed. A number of factors may have contributed to this, for example, the ratio of intact to remoulded penetration resistance (which is about 2 in these tests) was lower than what was typically encountered in the field (3 to 5 more typical for offshore clays). Another factor was the velocities and

frequencies of the motions used, which are about 4 times slower than those typically encountered in prototype situations. The choice of slower motions was dictated by the equipment capacity. Nonetheless, the topic of erosion scaling in centrifuge is a matter of further investigation.

The results demonstrated the trench geometry can have a significant influence on both bending and axial fatigue stresses in a riser. As the trench deepens the fatigue stresses appear to decrease. This decrease in fatigue stresses was about 20% for bending and up to 18% for axial. Base on these results it appears that deepening of the trench can potentially increase the fatigue life of a riser. These observations are in contrast to those reported by others based on tests on a segment of a pipe attempting to simulate riser-soil interaction (Giertsen et al., 2004; Leira et al., 2004) and numerical modeling (Shiri and Randolph, 2010).

4.7. ACKNOWLEDGEMENTS

We are grateful to Don Cameron, Derry Nicholl, and Karl Tuff for their contribution in the development and execution of the centrifuge tests, and to C-CORE for funding the test.

4.8. REFERENCES

Aubeny, C. P., and Biscotin, G., 2009, "Seafloor-Riser Interaction Model," *International Journal of Geomechanics*, 9(3), pp. 133-141.

- Elliott, B. J., Zakeri, A., Macneill, A., Phillips, R., Li, G., and Clukey, E. C., (submitted March 2012), "Centrifuge Modeling of Steel Catenary Risers at Touchdown Zone Part I: Development of Novel Centrifuge Experimental Apparatus," *Ocean Engineering* (under review).
- Finnie, I. M. S., and Randolph, M. F., 1994, "Punch-Through and Liquefaction Induced Failure of Shallow Foundations on Calcareous Sediments," *Proceedings International Conference on Behavior of Offshore Structures*, Boston, pp. 217-230.
- Giersten, E., Verley, R., Schroder, K., 2004. "CARISIMA A Catenary Riser/Soil Interaction Model for Global Riser Analysis," *International Conference on Offshore Mechanics and Arctic Engineering (OMAE2004)*, Vancouver, BC, Canada, pp. 633-640.
- Lehane, B.M., O'Loughlin, C.D., Gaudin, C., Randolph, M.F., 2009. "Rate Effects on Penetrometer Resistance in Kaolin." *Geotechnique* 59 (1), 41-52.
- Leira, B.J., Karunakaran, D., Giertsen, E., Passano, E., Farnes, K.A., 2004. "Analysis Guidelines and Application of a Riser-Soil Interaction Model Including Trench Effects," *International Conference on Offshore Mechanics and Arctic Engineering (OMAE2004)*, Vancouver, BC, Canada, pp. 955-962.
- Shiri, H., Randolph, M.A., 2010. "The Influence of Seabed Response on Fatigue Performance of Steel Catenary Risers in Touchdown Zone," *Proceedings of the ASME 2010 29th International Conference on Ocean, Offshore and Arctic Engineering*, OMAE2010, Shanghai, China.

5. CONCLUSIONS AND RECOMMENDATIONS

5.1. CONCLUSIONS

Advancing technology has made it possible for the development of deep-water reservoirs and the need for steel catenary risers. Literature review has shown fatigue in the touchdown zone is a main design parameter with limited knowledge surrounding the fatigue damage associated with the complex fluid-riser-soil interaction and trench formation in the TDZ.

Current SCR design is based on conservative simplified numerical models that use a rigid or linearly elastic seabed in the touchdown zone. Model complexity increases significantly as the trench formation mechanism is incorporated. The trench formation not only depends on the riser movement in the trench as a result of the vertical and lateral wave response, but is also believed to be based on the fluid (water) flow behaviour within the trench.

Limited large scale tests, such as STRIDE and CARISIMA, have attempted to study the different aspects of trench formation, such as the effect of heave and sway as well as soil degradation from vertical interaction, and the influence they have on the fatigue life of a riser. There are, however, still significant uncertainties in modeling the riser behaviour in the TDZ. Full-scale tests are very expensive and time consuming.

Centrifuge modeling is considered one of the most efficient and cost effective techniques for physically modeling various geotechnical problems in reduced time and space. In this study, the riser/seabed interaction has been modeled using the geotechnical centrifuge at C-CORE developing a unique experimental setup.

The development of the novel experimental centrifuge setup is presented in Chapter 3 of this thesis. Heave and surge wave loads can be applied simultaneously on the model riser that is fully instrumented. The apparatus is capable of simulating various motions of a semi-submersible vessel for wide range of frequencies. The first test was conducted on elastic seabed, which was verified using finite element modeling. It has been shown that centrifuge scaling laws can be successfully applied to simulate the complex engineering phenomenon of a SCR at TDZ. It is to be noted here that a number of successful tests have been conducted by other users using this apparatus under different client supported research programs.

Another successful test was conducted on soft clay seabed as typically encountered in deep sea. The seabed was prepared using kaolin clay. This test provided some valuable insights into various aspects of the fatigue issues related to the SCRs near the touchdown zone. The trench formation mechanism and its influence on the fatigue life, the fluid-riser-soil interaction, and pore pressure generated in the vicinity of the riser were successfully modeled.

The results demonstrated that the trench geometry could have a significant influence on both bending and axial fatigue stresses in a riser. As the trench curvature (i.e. geometry) changed and the depth increased, the fatigue stresses decreased. This decrease in fatigue stresses was about 20% for bending and up to 18% for axial. The change in trench curvature and increase in depth of the trench could potentially increase the fatigue life of a riser.

5.2.RECOMMENDATIONS

The present study shows that geotechnical centrifuge can be used for modeling the complex behaviour of soil/riser interaction in the touchdown zone. This was the first attempt of using a geotechnical centrifuge for modeling soil- riser interaction. There has been a large advancement in the understanding of the fatigue damage associated with the fluid-riser-soil interaction and trench formation in the touchdown zone through the development of this geotechnical tool; however, there is much to be learned. While the results show the expected trend, the results need to be further analyzed. One of the limitations was the modeling of erosion of soil around the trench, which may not be modeled properly using the current setup. Further investigation is required to resolve this issue. Another issue was the modeling of suction under the riser when it was lifted up. This may be resolved by numerical analyses supported by further testing. In summary, the trench formation mechanism was not fully understood from this study. Numerical study and more centrifuge tests under various seabed and loading conditions are required.

6. REFERENCES

- Aubeny, C. P., and Biscontin, G. (2009). "Seafloor-Riser Interaction Model," *International Journal of Geomechanics*, 9(3), pp. 133-141.
- Aubeny, C. P., Biscontin, G., and Zhang, J. (2006). "Seafloor Interaction with Steel Catenary Risers, Final Report." *OTRC Library Number: 9/06A173*. Texas A&M University, Austin. pp 1-22.
- Bridge, C., Howells, H., Toy, N., Parke, G., and Woods, R. (2003). "Full Scale Model Tests of a Steel Catenary Riser." *International Conference on Fluid Structure Interaction*, Cadiz, Spain.
- Bridge, C., Laver, K., Clukey, E., and Evans, T. (2004). "Steel Catenary Riser Touchdown Point Vertical Interaction Models." *Offshore Technology Conference (OTC 16628)*, Houston, Texas, USA. pp 1-7.
- Bridge, C., and Willis, N. R. T. (2002). "Steel Catenary Risers - Results and Conclusions from Large Scale Simulations of Seabed Interaction." *Deep Offshore Technology*, New Orleans, Louisiana, USA.
- Howells, H. (1995). "Advances in Steel Catenary Riser Design." *The 2nd Annual Deepwater Technology Conference*, Aberdeen, Scotland. pp 1-5.
- Hu, H. J. E., Chow, Y. K., Leung, C. F., Palmer, A. C. (2009). "Centrifuge Model Study of SCR Motion in Touchdown Zone." *Proceedings of the ASME 2009 28th International Conference on Ocean, Offshore and Arctic Engineering*, Hawaii, USA, OMAE2009-7928.

- Nakhaee, A., Zhang, J., (2010). "Trenching Effects on Dynamic Behavior of a Steel Catenary Riser". *Ocean Engineering* 37 (2-3), 277-288.
- Randolph, M., Quiggin, P. (2009). "Non-linear Hysteretic Seabed Model for Catenary Pipeline Contact". Proceedings of the ASME 2009 28th International Conference on Ocean, Offshore, and Arctic Engineering OMAE2009, Honolulu, Hawaii, USA.
- Pesce, C. P., Aranha, J. A. P., and Martins, C. A. (1998). "The Soil Rigidity Effect in the Touchdown Boundary Layer of a Catenary Riser: Static Problem." Eighth International Offshore and Polar Engineering Conference, International Society of Offshore and Polar Engineers, Montreal, Quebec, Canada.
- Sintef, M. (2001). "The CARISMA JIP: Catenary Riser/Soil Interaction Model for Global Riser Analysis (CARISIMA)."
"<http://www.sintef.no/Home/Marine/MARINTEK/MARINTEK-Publications/MARINTEK-Review-No-1---April---2002/CARISIMA---Catenary-RiserSoil-Interaction-Model-for-Global-Riser-Analysis/>", Cited on December 30, 2008.
- Thethi, R., and Moros, T. (2001). "Soil Interaction Effecton on Simple Catenary Riser Response." Deepwater Pipeline & Riser Technology Conference, Houston, Texas, USA.
- Willis, N. R. T., and West, P. T. J. (2001). "Interaction between Deepwater Catenary Risers and a Soft Seabed: Large Scale Sea Trials." Offshore Technology Conference (OTC 13113), Houston Texas, pp. 1-7

